Applied Catalysis B: Environmental 99 (2010) 388–397

Contents lists available at ScienceDirect

Applied Catalysis B: Environmental

journal homepage: www.elsevier.com/locate/apcatb

Photocatalytic oxidation of multicomponent mixtures of estrogens (estrone (E1), 17β-estradiol (E2), 17α-ethynylestradiol (EE2) and estriol (E3)) under UVA and UVC radiation: Photon absorption, quantum yields and rate constants independent of photon absorption

Gianluca Li Puma*, Valeria Puddu, Hin Kit Tsang, Alexander Gora, Bea Toepfer

Photocatalysis & Photoreaction Engineering, Department of Chemical and Environmental Engineering, The University of Nottingham, University Park, Nottingham NG7 2RD, United Kingdom

ARTICLE INFO

Article history:
Available online 21 May 2010

Keywords:
Endocrine disrupting chemical
Estrogens
Wastewater
Titanium dioxide
Degussa P-25
Quantum yield
UV radiation
Photocatalysis
Photolysis
Photoreactor
Suspensions
Radiation absorption
Radiation scattering
Radiation field
Reaction kinetics

ABSTRACT

The kinetics of photocatalytic degradation of multicomponent mixtures of four of the most powerful endocrine disrupting chemicals (estrogens) estrone (E1), 17β-estradiol (E2), 17α-ethynylestradiol (EE2) and estriol (E3) was studied in the presence and in the absence of TiO_2 (Degussa P25) suspensions. Experiments were carried out with UVA and UVC radiation in a well characterized annular photoreactor. The results were analysed in terms of a simple first-order kinetic model, but including the explicit effect of photon absorption. This was accomplished by modelling the radiation field under heterogeneous (photocatalysis) conditions and by determining the spatial distribution of the local volumetric rate of photon absorption (LVRPA) in the reactor. The Six-Flux Absorption-Scattering Model (i.e., scattered photons follow the route of the six directions of the Cartesian coordinates) using optical parameters averaged across the spectrum of the incident radiation was used to determine the LVRPA. The intrinsic reaction kinetic constants, of E1, E2, EE2 and E3, independent of reactor geometry and level of radiation absorbed within the reactor were determined under each different oxidation conditions. The quantum yields (moles of estrogens degraded per Einstein of photons absorbed) were estimated. The quantum yields under UVC-TiO_2 photocatalysis (2.1×10^{-3} to 3.9×10^{-3}) are on average double the yields under UVA-TiO_2 photocatalysis (1.2×10^{-3} to 1.8×10^{-3}).

The established model was found to be appropriate to predict the time-dependent degradation profiles of the estrogens in multicomponent systems. Using this simple approach, intrinsic kinetic data can be obtained.

1. Introduction

In recent years, there has been growing concern over the potential risk posed by natural and synthetic chemicals that can produce adverse effects on human and wildlife by interacting with the endocrine system [1,2]. These chemicals are generically named endocrine disrupters (ED) or endocrine disrupting chemicals (EDCs). Examples include natural and synthetic estrogens and xenoestrogens, which are a wide class of compounds including some pesticides and surfactants that can mimic the biological effect of estrogens.

Natural hormones and their metabolites have always been present in the natural environment. However, due to growing use of natural and synthetic estrogens in medicine and livestock farming, a rise in their occurrence in natural water systems has been observed [3,4]. A recent study on an experimental lake area [5] identified concerns over increasing feminisation of fish due to exposure to EDCs such as 17α-ethynylestradiol, present at very low concentration (ng/l) in the lake. Even at such low concentrations, steroid estrogens cause the synthesis and secretion of vitellogenin, a female specific protein, in male fish, resulting in induced sex reversal and/or intersexuality of fish population, and near extinction of fish in the lake.

Estrone (E1), 17-β-estradiol (E2), 17α-ethynylestradiol (EE2) and estriol (E3) are powerful natural estrogens which are commonly found in sewage treatment [6]. These estrogens are all 18-C steroids with a phenol moiety which is responsible for their estrogenic activity (Fig. 1). E2 is responsible for development of female secondary sex characteristic and reproduction and it shows the highest biological activity followed by EE2, E1 and E3.

* Corresponding author. Tel.: +44 0115 9514170; fax: +44 0115 9514115.
E-mail address: gianluca.li.puma@nottingham.ac.uk (G. Li Puma).

0926-3373/$ – see front matter © 2010 Elsevier B.V. All rights reserved.
doi:10.1016/j.apcatb.2010.05.015

Nomenclature

a	model parameter SFM
b	model parameter SFM
c_{cat}	photocatalyst concentration (kg m^{-3})
C_i	estrogen or substrate concentration (mol m^{-3})
C_{0i}	initial concentration of substrate i (kg m^{-3})
H	length of the reactor (m)
I	radiation intensity (or radiative flux) (W m^{-2})
I_λ	radiation intensity divided wavelength of radiation (W m^{-2} nm^{-1})
k_T	kinetic constant independent of radiation absorbed, units vary see Table 4
L	lamp length (m)
VRPA	volumetric rate of photon absorption (W or Einstein s^{-1})
LVRPA	local volumetric rate of photon absorption (W m^{-3} or Einstein m^{-3} s^{-1})
N	number of estrogens is solution
m	order of the reaction with respect to the LVRPA
p_b	probability of scattering in the backward direction
p_f	probability of scattering in the forward direction
p_s	probability of scattering in the side direction
r	radial coordinate (m)
r^*	dimensionless radial coordinate (=r/R)
r_l	lamp radius (m)
r_i	rate of the reaction with respect to substrate i (mol s^{-1} m^{-3})
R	external radius of annulus (m)
S_l	radiation emission of lamp per unit time per unit length (W m^{-1})
t	time (s)
V	total volume of fluid in recirculation system (m^3)
V_r	reactor volume (m^3)
z	axial coordinate (m)
z^*	dimensionless axial coordinate (=z/H)

Greek letters

α	geometrical parameter (=H/L)
β	geometrical parameter (=$L/\eta R$)
γ	dimensionless parameter SFM
δ	thickness of the annulus (m)
η	ratio of internal radius to external radius of annulus
κ	specific mass absorption coefficient averaged over the spectrum of the incident radiation (m^2 kg^{-1})
λ	radiation wavelength (m)
ξ	reaction space radial coordinate (m)
ξ^*	dimensionless reaction space radial coordinate (=ξ/δ)
σ	specific mass scattering coefficient averaged over the spectrum of the incident radiation (m^2 kg^{-1})
τ	optical thickness
τ_{app}	apparent optical thickness
φ	scattering angle
ϕ	quantum yield (mol Einstein^{-1})
Φ	scattering phase function
ω	scattering albedo (=$\sigma/(\sigma+\kappa)$)
ω_{corr}	corrected scattering albedo SFM

Subscripts

i	relative to substrate (estrogen) i
l	at the lamp wall
min	minimum
max	maximum
λ	wavelength
r, r^*	direction along the radial coordinate
ηR	position at inner wall of annulus
w	lamp wall
z, z^*	direction along the axial coordinate
0	position at inner wall of annulus

Superscript

*	dimensionless variable

Traditional methods of water treatment, such as activated sludge treatment, cannot be used to effectively remove these compounds from water effluents [7]. Currently, there are limited resources evaluating processes for estrogen removal from the environment [8], hence effective treatments are needed for estrogens remediation.

Direct photolysis and photocatalytic oxidation have been recently investigated as a mean of eliminating the estrogenic activity of these compounds [9–22]. The photolysis of estrone and 17-β-estradiol in aqueous solutions irradiated with UVC (lamp power 30 W) and UVA–vis (lamp power 125 W) radiation has been reported [16]. UVC radiation was found to be much more effective than UVA–vis. Estrone was photolysed at faster rate than 17-β-estradiol. The photolytic degradation was modelled by a pseudo first-order rate equation. It was suggested that the photolysis of E1 and E2 causes the rupture and oxidation of the benzene ring to produce compounds containing carbonyl groups.

In other studies [19,20] the rate of photocatalytic decomposition of 17-β-estradiol and estrone on TiO_2 immobilized on polytetrafluoroethylene mesh sheets was found to be mass-transfer controlled and fitted a pseudo first-order rate equation.

The photocatalytic degradation of 17-β-estradiol, in a 8 ml quartz reactor irradiated by a 150 W xenon lamp ($\lambda > 300$ nm) and containing 1.5 mg of TiO_2 (Degussa P25) immobilized on a 1 cm^2 Ti–6Al–4V alloy, was first reported by Coleman et al. [22]. The authors modelled the degradation kinetics using an apparent Langmuir–Hinshelwood kinetic rate equation. The same group more recently reported that photocatalytic oxidation is much more efficient than direct photolysis in the degradation of 17-β-estradiol, 17-α-ethynylestradiol and estrone [15]. The estrogens degrada-

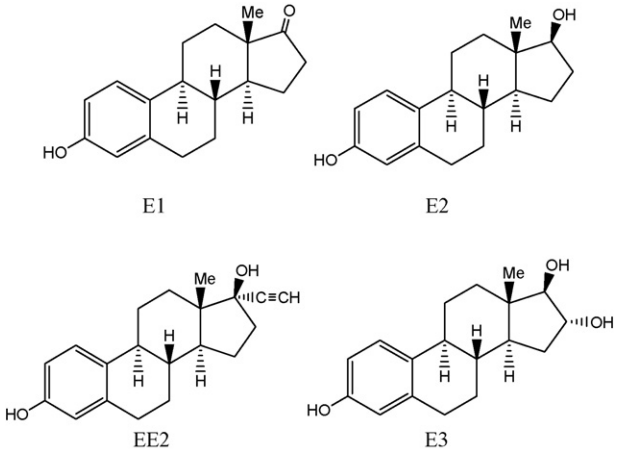

Fig. 1. Molecular structures of E1, E2, EE2 and E3.

tion kinetics were found to be first-order and photocatalysis was reported to be more effective than photolysis in the removal of the estrogenic activity of the steroids. In another study [21] it was shown that the estrogenic activity of 17-β-estradiol is removed concurrently with the initiation of photocatalytic degradation and that the estrogenic activities of the intermediates formed were negligible. The authors proposed a degradation mechanism which started with the hydroxylation of the phenol moiety in the molecule of 17-β-estradiol to yield, after a number of steps, 10ε-17-β-dihydroxy-1,4-estradiene-3-one and testosterone species, which were further mineralized to CO_2. The mechanism of photocatalytic degradation of 17-β-estradiol was further elucidated by Mai et al. [10].

The above studies clearly identify photocatalytic oxidation as a possible method for the elimination of the estrogenic activity of estrogen residues in water. They further established that it is not necessary to mineralize the entire molecule since the estrogenic activity is normally removed simultaneously with the degradation of the parent estrogen.

Recently, Zhang et al. [12] investigated the photodegradation of estrone and 17-β-estradiol in the presence of slurry suspensions of TiO_2 (Degussa P25) in the absence of oxygen purging. They investigated the effect of estrogens concentration, pH, catalyst concentration, humic acid concentration and hydrogen peroxide concentration in two different photoreactors. The reaction kinetics again was found to be pseudo first-order. However, the reaction rate constants determined in the two different reactors varied by 3-fold. Nakashima et al. [19] also reported rate constants of photodegradation of E1 and E2 up to one order of magnitude higher than in Zhang's work. The main reason for such large discrepancies is that the degradation rate constants of the estrogens were not decoupled from the volumetric rates of photon absorption (VRPA) occurring in each reactor configuration. As a result, this approach renders difficult the comparison of kinetic data among researchers and limits the use of such studies for design and optimization of photo(catalytic) reactors for water treatment.

In photolytic and photocatalytic oxidation processes, photon utilization efficiency is the primary factor which determines the effectiveness of the above processes. Therefore, an appropriate analysis of the photocatalytic degradation of estrogens should firstly be carried out in terms of quantum yield (moles of estrogens degraded per mole of photons absorbed). In this respect, a handful of data is available in the literature [14,22]. Furthermore, the correct kinetic analysis of photocatalytic reactions should account for the volumetric rate of photon absorption at each position of the reaction space irradiated by photons.

The kinetic parameters derived from the fitting of a kinetic model to the experimental results should be independent of the radiation absorbed in the reactor such that the model could be utilized for the design and scale-up of photoreactors of any size and shape. Such kinetic model would also allow an appropriate comparison of experimental results (e.g., kinetic constants) obtained in different photoreactors. These aspects are currently lacking in most studies in the literature and it is one of the reasons, in addition to photoreactor modelling, of why photoreactors are most often design by empirical or semi-empirical methods.

In this study, we investigate the kinetics of degradation of multicomponent mixtures of E1, E2, EE2 and E3 (Fig. 1) by UVA-photocatalysis and UVC-photocatalysis in slurry suspensions of TiO_2. Following accurate modelling of the radiation field in the photoreactor, we determine quantum yields (moles of estrogens degraded per mole of photons absorbed) for each of above oxidation processes. Furthermore, we estimate estrogens kinetic rate constants independent of the level of radiation absorbed within the photoreactor which assist in the elucidation the "true" reactivity of each estrogen under the different experimental conditions.

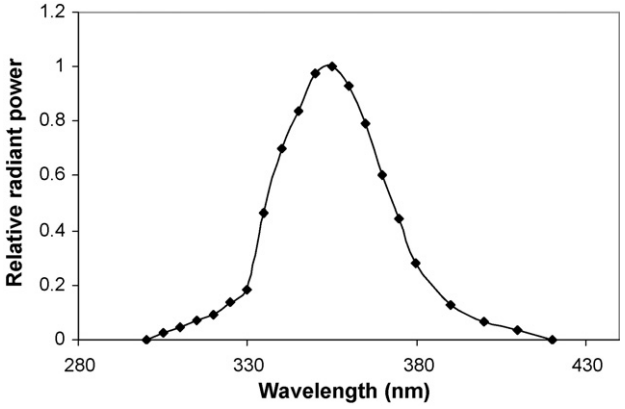

Fig. 2. Relative spectral power distribution of a Sylvania blacklight-blue F8W/BLB-T5 lamp.

2. Experimental

2.1. Materials

All chemicals were used as received without further purification. Estriol, estrone, 17β-estradiol (purity ≥ 97%) and 17-α-ethynylestradiol (purity ≥ 98%) were obtained from Sigma–Aldrich. The photocatalyst was TiO_2 (Degussa P25, primary particle size, 20–30 nm by TEM; specific surface area 52 $m^2 g^{-1}$ by BET; composition 78% anatase and 22% rutile by X-ray diffraction). For the HPLC analyses acetonitrile (E Chromasolv® for HPLC, far UV) was supplied by Riedel-de Haën. Ultra high purity water for all experiments and analyses was produced by a NANOpure Diamond UV water purification system that provides bacteria free water of 18.2 MΩ cm^{-1} resistivity with less than 1 ppb total organic carbon.

2.2. Photoreactor

The experiments were carried out in a well characterized annular photocatalytic reactor system that has been described elsewhere [23]. The reactor was operated in a recirculation batch mode, whereby reactants continuously passed through the reactor and were fed back to a well mixed recirculation tank. The outer wall of the photoreactor consists of a QVF borosilicate glass tube (internal diameter 0.038 m, wall thickness 0.0045 m), the inner wall is replaceable Pyrex or quartz tube (external diameter 0.026 m) mounted at the axial centre of the reactor. The radiation wavelength cut off by the Pyrex tube was found to be 300 nm. The length of the reaction zone in the annular photoreactor was 0.255 m. The irradiated volume of suspension (V_r) was 0.134 l. In the experiments using UVA radiation a Sylvania blacklight-blue F8W/BLB-T5 lamp was mounted axially inside the Pyrex tube. This lamp emits radiation in the 300–420 nm range with a peak at 355 nm. The emission spectrum of this UV lamp is shown in Fig. 2. In the experiments using UVC radiation a Philips TUV 8W lamp emitting radiation at 253.7 nm was mounted axially inside the quartz tube. Both types of lamps have identical dimensions and power (nominal power 8 W, bulb length 0.26 m, bulb diameter 0.0155 m). Each lamp was centred with respect to the axial length of the photoreactor. The lamps ends were covered with Teflon tape to leave a central section, 0.213 m in length, in which the radiation per unit length was found to be effectively constant. UV fluxes were measured using a microprocessor-controlled radiometer (Cole-Parmer) fitted with either a 254 nm UVC sensor or a 356 nm UVA sensor (sensors accuracy ± 5%; display accuracy ± 0.2% at full scale). The photon flux at

Table 1
Recovery rates of multicomponent mixtures of estrogens in the presence and in the absence of TiO_2.

Concentration (M)	Recovery rates in % (mean values)			
	E1	E2	EE2	E3
3.5×10^{-6} ($TiO_2 = 0\ g\ l^{-1}$)	96.8 ± 0.8	97.5 ± 1.1	99.1 ± 0.5	95.6 ± 1.4
3.5×10^{-6} ($TiO_2 = 0.4\ g\ l^{-1}$)	91.4 ± 1.6	90.3 ± 1.3	95.5 ± 0.9	90.7 ± 1.9

the wall of the UVC lamp was 113.5 W m^{-2}. The photon flux at the wall of the UVA lamp averaged across the emission spectrum of the UVA lamp (300 nm < λ < 380 nm for TiO_2) was estimated following the method in Li Puma et al. [24] and was found to be 115.6 W m^{-2}. Under the above experimental conditions, the lamp had identical dimensions and very similar photon emission fluxes.

2.3. Experimental procedures

Stock solutions of E1, E2, EE2 and E3 in acetonitrile at 100 mg l^{-1} were freshly prepared due to the poor solubility of the estrogens in water. They were diluted with ultrapure water to the desired concentration required for each experiment and or analysis. TiO_2 when used was added at a concentration of 0.4 kg m^{-3}. This catalyst concentration was found, experimentally, to be optimal for the present reactor/catalyst system [25]. Under these experimental conditions, the optical thicknesses of the photoreactor/catalyst system were 2.60 with UVA irradiation and 3.37 with UVC irradiation, which were within the optimal range for optimal radiation absorption [26].

All experiments were carried out using 2 l of estrogens suspension (V). In a typical experiment, the suspension was loaded to the recirculation tank, which was fitted with a mixing unit and an oxygen delivery system. The suspension was recirculated in the system using a pulse free peristaltic pump and equilibrated in the dark for 1 h. Irradiation of the suspensions started after that adsorption equilibrium between TiO_2 and estrogens was attained. The experiments were carried out at natural pH of the solution suspension. The initial pH was 4.6 ± 0.1 in the experiments in the presence of TiO_2 and 7.0 ± 0.3 in the experiments in the absence of TiO_2, and these values remained practically constant during the course of the reaction. Ultra high purity oxygen (99.999%, BOC gases, UK) was continuously supplied to the liquid in the recirculation tank during the experiments. The temperature was in the range of 22–24 °C.

2.4. Sample analysis

Samples collected at appropriate time intervals were filtered through 0.45 μm, 25 mm EasyDisc nylon filters (Whatman) to remove TiO_2 prior to solid phase extraction (SPE) and HPLC analysis. Separate HPLC analyses with filtered and unfiltered estrogens solutions confirmed that the filter material did not retain the analytes.

The OASIS® SPE Method for Estrogens in River Water (Endocrine Disruptors) reported by Waters was followed. OASIS® HLB Cartridges, 6 cm^3, 200 mg connected to an OASIS vacuum manifold system were used. The cartridges were initially conditioned with 3 ml of methyl t-butyl ether (MTBE) and then rinsed with 3 ml of methanol, followed by 3 ml of water. After loading of the samples, the cartridges were washed with 3 ml of 5% methanol in H_2O and allowed to dry, before eluting into clean test tubes with 6 ml of 10% methanol in MTBE. The elute was then evaporated to dryness under nitrogen gas and reconstituted to a final volume of 1 ml with 43% acetonitrile, 57% water. This was then transferred to vials and analysed by HPLC.

Table 1 shows the recovery rates of multicomponent mixtures of the four estrogens in the presence and absence of catalyst. 95% estrogens recovery rates or higher were obtained with the above method. It also shows that approximately 5% of estrogens adsorbs onto the catalyst.

The HPLC system (Agilent 1100 series) comprised a diode array detector a mobile phase degassing unit and an autosampler. The optimization of the analytical method resulted in the following operating conditions: Supelcosil LC-8 (4.6 mm × 250 mm, 5 μm) column supplied by Supelco, mobile phase 43% acetonitrile, 57% water, flow rate 1 ml min^{-1}, column temperature 15 °C, detector wavelengths 200 and 280 nm. The analytes retention times were 4.2 min for E3, 7.7 min for E2, 9.0 min for EE2 and 9.6 min for E1. Calibration of the HPLC chromatographic peaks against standards of the estrogens in acetonitrile resulted in a linear response in the range of concentrations investigated (10^{-6} to 10^{-9} M). The smallest quantifiable chromatographic peak after SPE corresponded to approximately 3 nM for each estrogens.

3. Results and discussion

3.1. Degradation kinetics of estrogens

Fig. 3 shows the degradation profiles against irradiation time of near equimolar solutions of E1, E2, E3 and EE2 when the solution

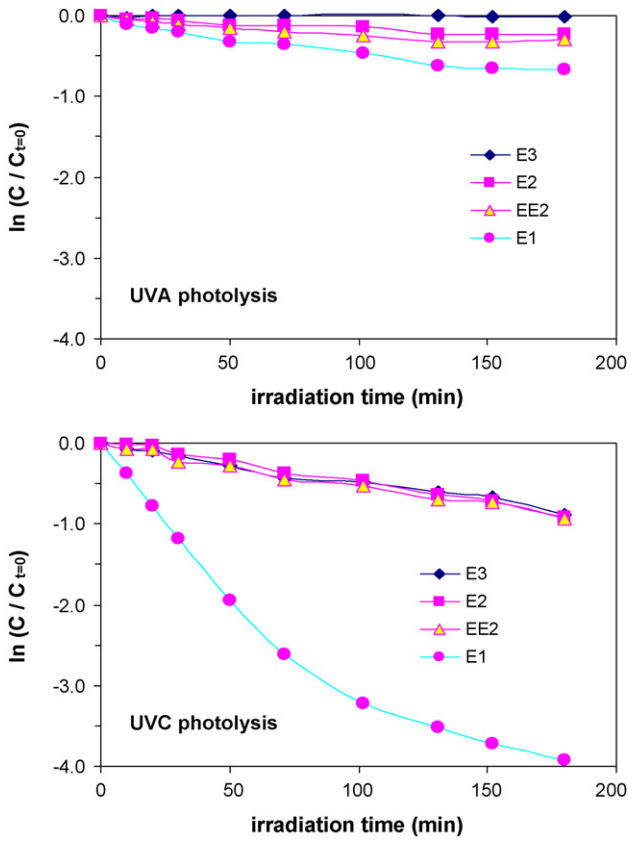

Fig. 3. Degradation of near equimolar solutions of E1, E2, E3 and EE2. (a) UVA photolysis: $C_{t=0}$ (μM), E1 = 3.24, E2 = 2.98; EE2 = 3.28; E3 = 3.54. (b) UVC photolysis: $C_{t=0}$ (μM), E1 = 3.04, E2 = 2.81; EE2 = 3.05; E3 = 3.63.

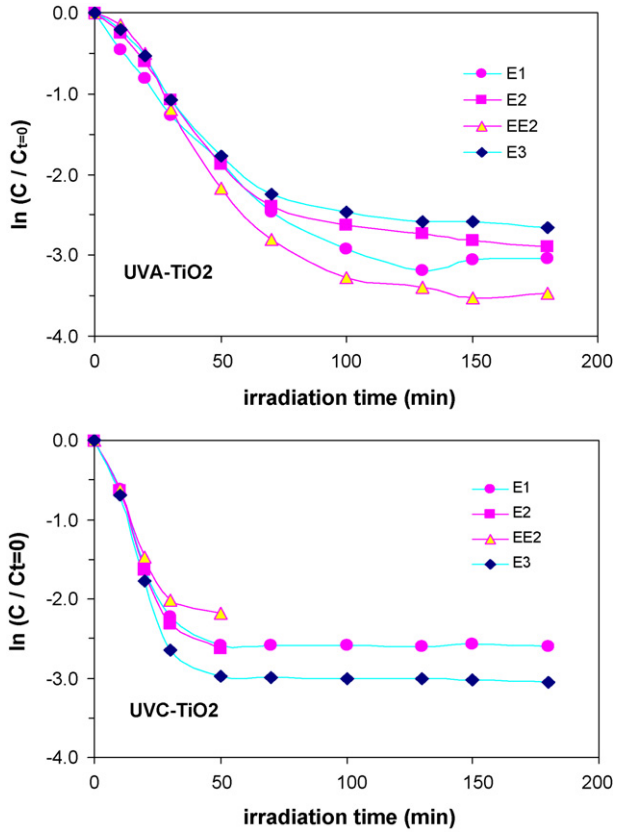

Fig. 4. Degradation of near equimolar solutions of E1, E2, E3 and EE2. (a) UVA-TiO_2: $C_{t=0}$ (μM), E1 = 3.76, E2 = 2.42; EE2 = 3.00; E3 = 3.59. (b) UV-TiO_2: $C_{t=0}$ (μM), E1 = 2.92, E2 = 2.54; EE2 = 3.07; E3 = 3.67.

was irradiated with either UVA or UVC radiation, in the absence of catalyst (photolysis). The degradation of estrogens follows apparent first-order kinetics other than for E1 in Fig. 3b, which deviates after a 3-ln decrease in concentration. Under UVA irradiation, the degradation of E3 was not significant, however, E1, E2 and EE2 were removed reaching respectively 49, 20 and 25% conversion after 180 min of irradiation. Under UVC irradiation, the rate of degradation of estrogens in the mixture increased significantly. The conversions of E2, EE2 and E3 after 180 min were 60%, but reaction was much faster for E1, which was almost completely degraded (98% conversion). The faster degradation of the estrogens under UVC irradiation can be explained by their much stronger absorption of photons in the UVC region of the electromagnetic spectrum (see Section 3.3).

The degradation sequence observed in Fig. 3 with a multicomponent solution of estrogens, follows the sequence E1 > EE2 > E2 > E3, which is in agreement with the results reported for single component experiments for E1 and E2 [16]. It was shown that E1 photolysed at much faster rate than E2 under both UVC radiation and UVA–vis radiation. Conversely, in another work with immobilized TiO_2 on titanium alloy in which mass-transfer limitations may have occurred, the degradation rate under UVA photolysis was found to be EE2 > E1 > E2 [15], which contrasts for E1 with the results in Fig. 3a, obtained in a slurry TiO_2 suspension.

Fig. 4 shows the degradation profiles of near equimolar solutions of E1, E2, E3 and EE2 in the presence of TiO_2, when the solution was irradiated with either UVA or UVC radiation. Under these conditions radical species (e.g., hydroxyl) are formed on the surface of TiO_2 and these react with the estrogens adsorbed onto the surface. With UVA radiation, degradation of estrogens occurs primarily by photocatalysis since the absorption of photons by the TiO_2 slurry suspension vastly exceed, the absorption of radiation by the molecules in solution. The Napierian absorption coefficient of a 0.4 g/l TiO_2 suspension averaged across the radiation emission spectrum of the UVA lamp (Fig. 2) was estimated to be 135.2 m^{-1}. This value exceeded the spectral averaged Napierian absorption coefficient of the estrogens in solution by at least 4 orders of magnitude. Therefore, the photolysis of the estrogens in the presence of UVA irradiation and TiO_2 was insignificant. The rates of photocatalytic degradation of the estrogens under irradiation of TiO_2 with UVA were much higher than the rates under UVC photolysis. In the initial phase of the degradation, up to 2 or 3-ln decrease in estrogens concentrations, the degradation of estrogens follows apparent first-order kinetics. However, higher estrogens conversions were achieved at much slower degradation rates. It has been reported that refractory intermediates from E2 may be formed [10], however, this aspect is unclear and needs further investigation.

With UVC radiation and Ti_2, photolysis of the estrogens may be complementary to photocatalysis and the degradation of the estrogens was even faster (Fig. 4). The estrogens also degrade at similar rates indicating that the main reaction mechanism might occur under heterogeneous conditions. The identification of reaction intermediates and reaction mechanisms involved under each of the above oxidation conditions have been treated elsewhere [10,16,21]. Although much work needs to be done in this area, this aspect of research was not the main purpose of the present work. Here, instead we explain the observed estrogens degradation rates by calculating the quantum yields under each of the above experimental conditions and, in addition, reaction rate constants independent of photon absorption in the reactor. Since the absorption of photons and the volumetric rate of photon absorption (VRPA) in the reaction space differ in each of the above oxidation methods, the results from simple degradation experiments are not conclusive to elucidate the reactivity of each estrogen under the different photooxidation conditions. The quantum yield (moles of estrogens degraded per mole of photons absorbed) should first be estimated, and this is not a trivial task especially when absorption and scattering of photons take place in the presence of a solid photocatalyst [27].

In the present study, the quantum yield of degradation for each estrogen was estimated from the initial reaction rate as follows:

$$\phi = \frac{V(dC_i/dt)_{t=0}}{\text{VRPA}} \quad (1)$$

where (dC_i/dt) is initial rate of degradation of each estrogen determined from the experiments, V is the volume of liquid and VRPA is the volumetric rate of photon absorption in the reaction space.

3.2. Estimation of the volumetric rate of photon absorption (VRPA)

As a result of the irreducible heterogeneity of the radiation field in the reactor, the estimation of the VRPA in the reactor space requires the integration of the local volumetric rate of photon absorption (LVRPA) throughout the reactor volume (V_r):

$$\text{VRPA} = \int_{V_r} (\text{LVRPA})\ dV_r \quad (2)$$

The LVRPA is the photon energy absorbed at a specific position in the reaction space. In homogenous reaction systems, with no catalyst, the LVRPA is determined by the absorption of the species in solution. Conversely, in the presence of TiO_2 particles in suspension the expression of the LVRPA would need to consider the absorption of photons by both the catalyst and the species in solution. However, since the concentration of estrogens in solution is very small, the absorption of estrogens is several orders of magnitude smaller than that of TiO_2, therefore, the contribution from the species in solution to the LVRPA can be safely neglected. This is not the case

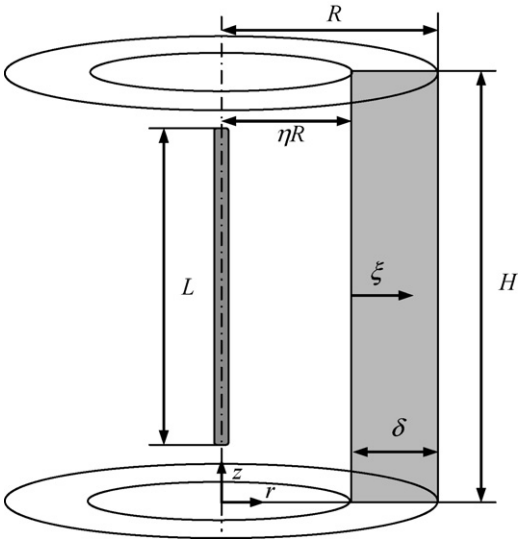

Fig. 5. Schematic representation of the geometry of an annular photocatalytic reactor. L is the lamp length, H is the reactor length and R is the outer radius if the annulus.

when considering the effect of direct photolysis on the estrogens degradation kinetics (Fig. 4).

3.2.1. LVRPA in heterogeneous systems

In a heterogeneous system transport of photons is governed by absorption, scattering and emission. The calculation of the spatial distribution of the LVRPA in a suspension of TiO_2 particles requires solving the radiative transfer equation (RTE) in the reaction space [28]. However, the mathematical analysis needed to solve the RTE can be demanding, especially to non-experts and in complex reactors. A simpler approach for the analytical determination of the LVRPA through the solution of differential photon balances has been reported [24,26,29]. This model, named Six-Flux Absorption-Scattering Model (SFM) solves the RTE considering photon scattering probabilities, without abandoning the essentials features of a rigorous approach. The SFM has been successfully applied to annular photoreactors modelling with single [24,30] and multicomponent [25] systems of herbicides and to flat heterogeneous reactors [29]. In this work the LVRPA was estimated by the SFM.

The SFM takes into account both absorption and scattering of photons which occur in the reaction space in which the suspension of photocatalytic particles flows. With relation to the annular photocatalytic reactor in this work, the following assumptions were made: uniform distribution of photocatalytic particles in the suspension and invariant optical characteristics; negligible absorption of energy by the fluid or the reactor walls; the wavelength of the absorbed photons was less than 384 nm (TiO_2 anatase band-gap); photons of energy higher than the band-gap of the semiconductor are either absorbed or scattered upon colliding with a photocatalytic particle and scattering follows the route of one of the six directions of the Cartesian coordinates; geometric optics was applied.

The LVRPA at a point (r, z) in the reaction space calculated with the SFM in cylindrical coordinate, for an infinitely long annular photocatalytic reactor (Fig. 5), is [26,31]:

$$\mathrm{LVRPA} = \frac{\tau_{app} I_{(\eta R),z^*}}{\omega_{corr}(1-\gamma)(1-\eta)R} \times \frac{\eta}{[\eta+(1-\eta)\xi^*]} \times \left[\left(\omega_{corr} - 1 + \sqrt{1-\omega_{corr}^2}\right) \exp(-\tau_{app}\xi^*) + \gamma\left(\omega_{corr} - 1 - \sqrt{1-\omega_{corr}^2}\right) \exp(\tau_{app}\xi^*)\right] \quad (3)$$

where ξ^* is the dimensionless radial coordinate in the reaction space ($=\xi/\delta$), η is the ratio between the radius of the inner and outer wall of the annulus, τ_{app} is the apparent optical thickness,

$$\tau_{app} = a\tau\sqrt{1-\omega_{corr}^2} \quad (4)$$

τ is the optical thickness,

$$\tau = (\sigma+\kappa)c_{cat}\delta = (\sigma+\kappa)c_{cat}R(1-\eta) \quad (5)$$

and a, b, ω_{corr} and γ are SFM parameters,

$$a = 1 - \omega p_f - \frac{4\omega^2 {p_s}^2}{1-\omega p_f - \omega p_b - 2\omega p_s} \quad (6)$$

$$b = \omega p_b + \frac{4\omega^2 {p_s}^2}{1-\omega p_f - \omega p_b - 2\omega p_s} \quad (7)$$

$$\omega_{corr} = \frac{b}{a} \quad (8)$$

$$\gamma = \frac{1-\sqrt{1-\omega_{corr}^2}}{1+\sqrt{1-\omega_{corr}^2}} \exp(-2\tau_{app}). \quad (9)$$

ω is the scattering albedo defined as

$$\omega = \frac{\sigma}{\sigma+\kappa} \quad (10)$$

where σ and κ are the specific mass scattering and absorption coefficients, respectively, which for polychromatic radiation can be averaged over the useful spectrum of the incident radiation:

$$\sigma = \frac{\int_{\lambda_{min}}^{\lambda_{max}} \sigma_\lambda I_\lambda \, d\lambda}{\int_{\lambda_{min}}^{\lambda_{max}} I_\lambda \, d\lambda} \quad (11)$$

$$\kappa = \frac{\int_{\lambda_{min}}^{\lambda_{max}} \kappa_\lambda I_\lambda \, d\lambda}{\int_{\lambda_{min}}^{\lambda_{max}} I_\lambda \, d\lambda}. \quad (12)$$

λ_{min} and λ_{max} are the minimum and maximum wavelengths of the incident radiation that can be absorbed by the photocatalyst (e.g. for TiO_2 Degussa P25, $\lambda_{max} = 380$ nm).

The apparent optical thickness τ_{app} of the reaction space is related to the "characteristic extinction length" of photons when radiation scattering is present and is related to the optical thickness, which would be measured using a "geometrically thick" photoreactor system with scattering particles.

The model parameters p_b, p_f and p_s of the SFM are the probability of backward, forward and side scattering, respectively. They can be estimated by fitting the SFM to the exact solution of the radiative transfer equation by the Monte Carlo approach. Assuming a "diffusively reflecting large sphere" phase function of radiation scattering [32] given by:

$$\Phi(\varphi) = \frac{8}{3\pi}(\sin\varphi - \varphi\cos\varphi), \quad (13)$$

p_b, p_f and p_s are equal to 0.71, 0.11 and 0.045, respectively [29]. Other scattering phase functions, including isotropic scattering (i.e., p_b, p_f and $p_s = 1/6$ for SFM) or the Henyey and Greenstein function [33] may be proposed, however, for the purpose of the present work, Eq. (13) was adopted. In reality, the procedure is independent of the choice of a particular phase function, and may be easily adapted to any phase function by simply adjusting the values of the three parameters p_b, p_f and p_s.

3.2.2. Incident photon flux

$I_{(\eta R),z^*}$ in Eq. (3) is the radiation flux at the inner wall of the annulus entering perpendicularly to the reactor wall, which varies along the axial direction. To estimate this flux in a simple way, the cylindrical UV lamp was modelled as a line source with each point

Table 2
Optical parameters of the TiO_2 suspension and system parameters.

Model parameter	Irradiation with UVA lamp	Irradiation with UVC lamp
Useful emission wavelength	300–380 nm	253.7 nm
Scattering albedo, ω	0.74	0.4
Specific absorption coefficient, κ	338 $m^2\ kg^{-1}$	1010.3 $m^2\ kg^{-1}$
Specific scattering coefficient, σ	964 $m^2\ kg^{-1}$	673.5 $m^2\ kg^{-1}$
TiO_2 catalyst loading	0.4 $kg\ m^{-3}$	0.4 $kg\ m^{-3}$
Optical thickness, τ	2.60	3.37
Apparent optical thickness, τ_{app}	1.89	3.07
Geometrical parameters	$\alpha = 1.197$, $\beta = 16.385$	$\alpha = 1.197$, $\beta = 16.385$

of the line emitting radiation in every direction and isotropically (linear source spherical emission, LSSE, model, [34]). Since the UV lamp ends were blanketed with tape, the radiation emitted by each point of the lamp was effectively constant along the axial length of the lamp. The lamp was located in the centre of the annulus of the photoreactor, and no radiation absorption, scattering or emission in the space between the lamp and the inner wall of the annulus occurred.

Under the above assumptions, the incident photon flux entering the inner wall of the reactor is [35]:

$$I_{(\eta R),z^*} = \frac{S_l}{4\pi\eta R}\left\{\arctan\left[\frac{\beta}{2}(2\alpha z^* - \alpha + 1)\right] - \arctan\left[\frac{\beta}{2}(2\alpha z^* - \alpha - 1)\right]\right\} \quad (14)$$

where S_l is the radiation emission of the lamp per unit time and unit length of the lamp,

$$S_l = 2\pi r_l \int_{\lambda_{min}}^{\lambda_{max}} I_{w,\lambda}\, d\lambda = 2\pi r_l I_w \quad (15)$$

α and β are the geometrical design parameters of an annular photoreactor,

$$\alpha = \frac{H}{L} \quad (16)$$

$$\beta = \frac{L}{\eta R}, \quad (17)$$

and z^* is the dimensionless axial coordinate,

$$z^* = \frac{z}{H} \quad (18)$$

It should be noted that, according to Eq. (14), the incident photon flux is not uniform along the entire length of the reactor.

The SFM described above was derived under the assumption that the intensity of the incident radiation at the inner wall was approximately constant for an axial length of the reactor equal to the thickness of the annulus. In addition, the average travelling path length of scattered photons in the axial direction before they become extinguished by absorption was always much less than the thickness of the annulus. These assumptions are rational for an annular photocatalytic reactor of optimal geometry, i.e., the geometrical design parameter α and β have been selected such that the axial change in $I_{(\eta R),z^*}$ is small for the majority of the length of the reactor (i.e., $\alpha = 1.2$ and $\beta = 16.4$ for the present reactor) and that it is operating at optimal optical thicknesses ($\tau_{app} > 1$).

3.3. Model parameters

The optical properties of TiO_2 (Degussa P25) in suspension were estimated following the method reported previously [24] and under the prevailing condition of mixing and particle agglomeration in the reactor. These conditions differ considerably with respect to optical properties measured with sonicated suspensions of TiO_2 [33]. Table 2 summarises the optical properties of TiO_2 when the reactor was operated with the UVA lamp and when it was operated with the UVC lamp. A much higher degree of photon absorption and less radiation scattering was observed under UVC radiation.

The molar absorption coefficients of the estrogens at 253.7 nm were measured spectrophotometrically in the linear region of the Beer–Lambert's law and the results are shown in Table 3. In the wavelength region emitted by the UVA lamp the absorption coefficients of the estrogens were found to be negligible.

3.4. LVRPA radial profiles and VRPA

The UVC and UVA lamps used in the experiments were of the same power rating and emitted approximately the same photon flux. However, the LVRPA in the reactor in the presence of a TiO_2 slurry suspension were different. The radial profiles of the LVRPA in the middle of the reactor ($z^* = 0.5$), estimated using the radiation models described above for the conditions in Table 2 are shown in Fig. 6. The UVC-photocatalytic process yields the highest values of the LVRPA in the reactor space, which is a consequence of the lower scattering albedo of TiO_2 in the UVC region compared with that in the UVA region (Table 2).

By integrating the LVRPA across the entire volume of the reactor (Eq. (2)) the VRPA was obtained.

The VRPA reported in Table 4 was estimated under the different oxidation conditions using the models described above with the parameters from Table 2. It should be noted that, under the

Table 3
Specific absorption coefficients of estrogens at 253.7 nm.

Estrogen	($M^{-1}\ cm^{-1}$)
Estrone (E1)	395.17
17-β-Estradiol (E2)	386.25
17-α-Ethynylestradiol (EE2)	314.62
Estriol (E3)	234.16

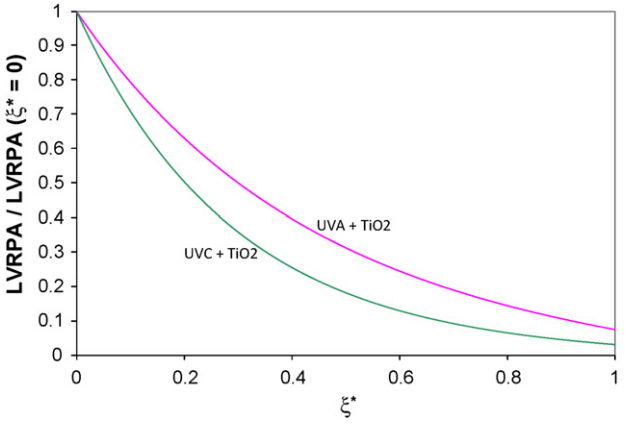

Fig. 6. Normalized radial profiles of the LVRPA for each photooxidation process, in the middle of the reactor ($z^* = 0.5$), as predicted by the radiation models for the conditions in Tables 2 and 3. LVRPA ($\xi^* = 0$) is 24035 $W\ m^{-3}$ for the UVA photocatalytic process and 48559 $W\ m^{-3}$ for the UVC-photocatalytic process.

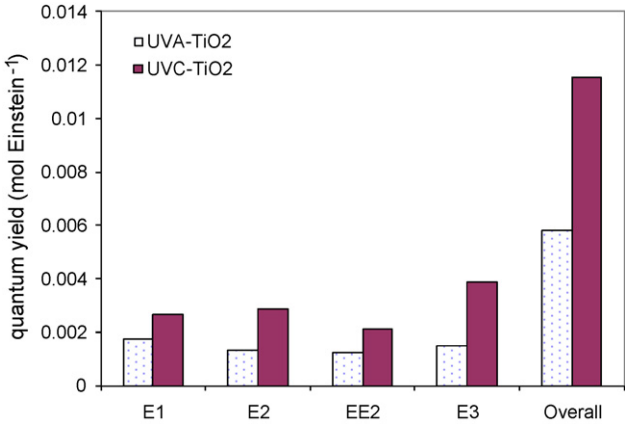

Fig. 7. Quantum yields of near equimolar solutions of E1, E2, E3 and EE2 when irradiated with either UVA (VRPA = 2.62×10^{-6} Einstein s^{-1}) or UVC (VRPA = 2.74×10^{-6} Einstein s^{-1}) radiation in the presence of TiO_2 (0.4 g l^{-1}).

experimental conditions used, the absorption of UVC radiation by the estrogens in solutions is 1585 times less than the absorption of radiation by the TiO_2 suspension. As a result, the absorption of radiation by the estrogens in solution was neglected in the calculation of the VRPA for the UVC–TiO_2 process.

3.5. Estrogens quantum yields

The quantum yield of each estrogen in the mixture was estimated from the initial reaction rate (Eq. (1)).

Fig. 7 shows the quantum yields of near equimolar solutions of the estrogens when irradiated with either UVA or UVC radiation in the presence of TiO_2. The quantum yields under UVC-TiO_2 photocatalysis are on average double the yields under UVA-TiO_2 photocatalysis. The VRPA in Einstein s^{-1} with the two configurations were approximately the same (Table 2) which implies that similar amounts of electron–hole charges were generated in both the UVA-TiO_2 and UVC-TiO_2 systems. Therefore, differences in photons absorption do not explain the differences in quantum yields noted in Fig. 7. Several reasons may be proposed as follows:

(a) A certain degree of estrogens photolysis in the UVC-TiO_2 system may occur, although the degradation curves shown in Figs. 3b and 4 do not appear to be additive. Considering the first 30 min of reaction time in Fig. 4, the rate increase of estrogens degradation from the results for UVA-TiO_2 and the results for UVC-TiO_2 systems is larger than the contribution from photolysis reported Fig. 3b. Furthermore the faster degradation of E1 (Fig. 3b) is not reflected in faster E1 degradation in Fig. 4b.
(b) UVC radiation may photolyse absorbed impurities on TiO_2 and "clean" the surface for adsorption of reacting species.
(c) The reduced probability of electron–hole recombination due to shorter penetration distance of 253.7 nm photons into the particle of TiO_2 might may cause an increase of trapped electron–hole couples and therefore of the concentration of the active oxidizing species at the surface of the catalyst. A fundamental mechanistic study would be required to identify the reasons and if there are synergistic interactions between photocatalysis and photolysis.

Table 4
Volumetric rate of photon absorption with different oxidation conditions.

Reactor operating conditions	VRPA (W)	VRPA (Einstein s^{-1})
UVA lamp, TiO_2 = 0.4 g l^{-1}	0.888	2.62×10^{-6}
UVC lamp, TiO_2 = 0.4 g l^{-1}	1.290	2.74×10^{-6}

The quantum yields reported in Fig. 7 when compared to those from UVC photolysis in literature are at least one order of magnitude lower. For example, the quantum yields of E2 and EE2 photolysis at 254 nm have been reported in the range from 0.026 and 0.067 [14,36]. This last result is significant since it demonstrates that photolysis is a more efficient process than photocatalysis in the degradation of estrogens when the comparison is made in terms of number of molecules transformed relative to the number of photons absorbed. The UVC excitation of the phenolic ring of the estrogens in solution results in photoproducts arising from a further reactivity of the carbon in position 17 [36]. In contrast, the photocatalytic degradation mechanism involves, electron–hole recombination, multiple reaction steps and back reactions which may hinder the quantum yield.

The results in Fig. 7 further show that in the presence of TiO_2 the quantum yield follows the sequence E3 > EE2 > E1 > E2, although the difference was not significant among the estrogens. In comparison, Coleman et al. [22] reported a quantum efficiency (not yield) of degradation of E2 under UVA on an immobilized TiO_2 film which was 16.9-fold smaller than the quantum yield of E2 in the present study. It shows that reactors using slurry suspensions of TiO_2 have the lead to reactors utilizing immobilized catalysts for the removal of estrogens.

3.6. Kinetic model and reaction rate constants

Current studies in the literature on estrogens photo(catalytic) degradation, report first-order kinetics [9,11–22]. However, none of these give rate constants which are independent of photon absorption effects. In other words, the rate constants determined in these work belong to the reactor set up, geometry and level of irradiation utilized, since they have not been decoupled from the actual amount of radiation absorbed by the reacting species and/or catalyst. In the present work, we estimate rate constants of estrogens photo(catalytic) degradation which are independent of the radiation absorbed within the photoreactor. The degradation kinetics of estrogens in the first 2 or 3-ln reduction in concentration (Fig. 4) can be fitted by apparent first-order kinetics. The reaction rate of each estrogen in solution can be modelled by:

$$-r_i = k_{T,i}(\mathrm{LVRPA})^m C_i \tag{19}$$

where $k_{T,i}$ is an apparent reaction rate constant which is independent of photon absorption in the reactor. The exponent m is equal to 0.5 in the presence of TiO_2 as shown previously for the oxidation of pesticides in the same reactor and under identical experimental conditions [25]. It should be noted that for slow photocatalytic oxidation kinetics such as with pesticides and estrogens, the value of m should be relatively independent on the type of substrate. Instead, it should be dependent on the radiation intensity level over the catalyst. A half-order dependence of the pollutant degradation rate from the LVRPA is obtained when the rate of electron–hole recombination in TiO_2 particles becoming predominant over the pollutant photocatalytic rate over its surface.

In order to represent the full dynamic behaviour of the present recirculation reaction system, which has total volume (V) and reactor volume (V_r), the rate equations were combined with the material balance and Eq. (2) to yield the following differential equation(s):

$$V\frac{dC_i}{dt} = -k_{T,i}C_i \int_{V_r} (\mathrm{LVRPA})^m \, dV_r \quad i = 1, 2, \ldots, n \tag{20}$$

Table 5
Reaction rate constants (Eq. (19)) of estrogens photooxidation in the presence of TiO_2.

	E1	E2	EE2	E3
UVA-TiO_2				
$k_{T,i}$ ($m^{1.5}\ s^{0.5}\ J^{-1.5}$)	1.378×10^{-6}	1.313×10^{-6}	1.506×10^{-6}	1.240×10^{-6}
$k_{T,i}$ ($m^{1.5}\ s^{0.5}$ Einstein$^{-1.5}$)	0.466	0.444	0.509	0.420
UVC-TiO_2				
$k_{T,i}$ ($m^{1.5}\ s^{0.5}\ J^{-1.5}$)	1.932×10^{-6}	2.003×10^{-6}	1.772×10^{-6}	2.250×10^{-6}
$k_{T,i}$ ($m^{1.5}\ s^{0.5}$ Einstein$^{-1.5}$)	0.910	0.943	0.835	1.060

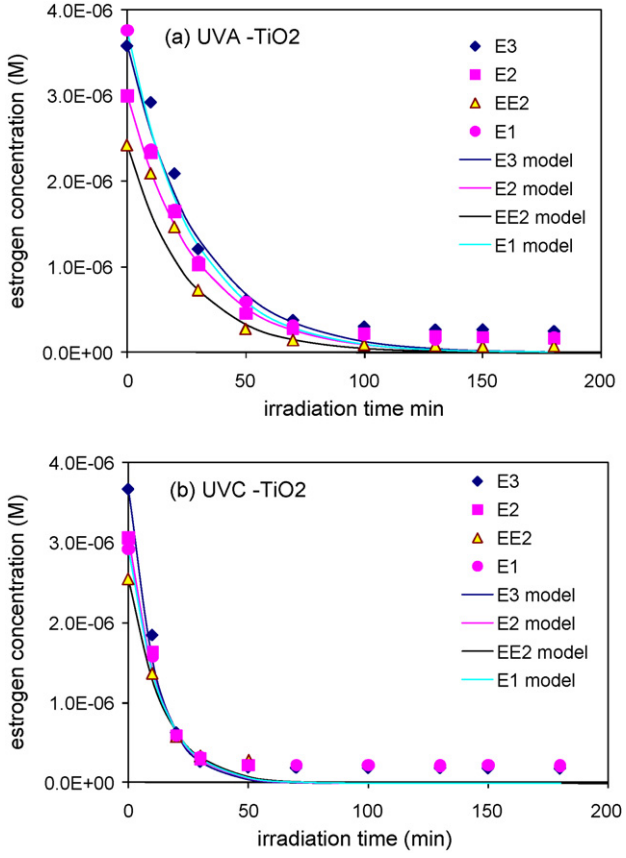

Fig. 8. Degradation of a multicomponent mixture of estrogens. Comparison between experimental and model prediction (Eq. 24, with model parameters from Tables 4 and 5) for (a) UVA-TiO_2 and (b) UVC-TiO_2.

which can be integrated using the initial condition(s) ($t = 0$, $C_j = C_{0j}$) to yield the time-dependent degradation profile of each estrogen.

$$C_i = C_{0i}\ \exp\left(-\frac{k_{T,i}\int_{V_r}(\mathrm{LVRPA})^m\ dV_r}{V}\times t\right) \tag{21}$$

or

$$\ln\frac{C_i}{C_{0i}} = -\frac{k_{T,i}\int_{V_r}(\mathrm{LVRPA})^m\ dV_r}{V}\times t \tag{22}$$

The integral in Eq. (21) can be evaluated using the radiation model described earlier with $m = 0.5$ for photocatalytic oxidation. The apparent rate constants $k_{T,j}$ displayed in Table 5 were evaluated from fitting Eq. (22) to the linear portion of the results in Fig. 4. These rate constants are independent of photon absorption effects in the reactor, therefore, they can be used together with the rate law Eq. (19) to represent the kinetics of degradation of the estrogens under study in photoreactors of different size and geometry and under different levels of irradiation.

The quality of the fitting of the time-dependent concentration profiles of estrogens degradation under the different oxidizing conditions is shown in Fig. 8. It shows that, the main trend of estrogens removal is captured satisfactorily, at least up to 85% conversion, in the region where first-order degradation kinetics holds.

4. Conclusions

This work has shown the significance of modelling the radiation field in photo(catalytic) reactors and of determining kinetics rate constants independent of reactor geometry and radiation field in the reactor. It has applied these concepts to the degradation of environmentally significant pollutants, such as four of the most common and powerful estrogens found in water and wastewater. Following an accurate modelling of radiation absorption and scattering in the photoreactor by the SFM, it was possible to estimate true quantum yields and derive kinetic parameters that are independent of the radiation field in the photoreactor. As a result, the rate laws and kinetic parameters are transferable among reactors and could also be used to the design, scale-up and optimization of industrial photocatalytic purification systems. In addition, the method described should allow the comparison of catalysts activities among researchers utilizing different reactor configurations.

It is hoped that the methodology described in this paper will be followed by researchers in photochemistry and photocatalysis, to assist them in the estimation of the true activity of photocatalytic materials, either commercial ones or self-synthesized.

Acknowledgements

The authors are grateful to NATO (Grant CPB.EAP.SFPP 982835) and the EU Socrates-Erasmus Programme for the financial support to produce this work.

References

[1] J.G. Vos, E. Dybing, H.A. Greim, O. Ladefoged, C. Lambre, J.V. Tarazona, I. Brandt, A.D. Vethaak, Crit. Rev. Toxicol. 30 (2000) 71.
[2] T. Colborn, F.S. Vom Saal, A.M. Soto, Environ. Health Perspect. 101 (1993) 378.
[3] T.A. Hanselman, D.A. Graetz, A.C. Wilkie, Environ. Sci. Technol. 37 (2003) 5471.
[4] T.A. Ternes, M. Stumpf, J. Mueller, K. Haberer, R.-D. Wilken, M. Servos, Sci. Total Environ. 225 (1999) 81.
[5] K.A. Kidd, P.J. Blanchfield, K.H. Mills, V.P. Palace, R.E. Evans, J.M. Lazorchak, R.W. Flick, PNAS 104 (2007) 8897.
[6] C. Desbrow, E.J. Routledge, G.C. Brighty, J.P. Sumpter, M. Waldock, Environ. Sci. Technol. 32 (1998) 1549.
[7] A.C. Johnson, J.P. Sumpter, Environ. Sci. Technol. 35 (2001) 4697.
[8] K.K. Koh, T.Y. Chiu, A. Boobis, E. Cartmell, M.D. Scrimshaw, J.N. Lester, Environ. Technol. 29 (2008) 245.
[9] Y. Zhang, J.L. Zhou, Chemosphere 73 (2008) 848.
[10] J. Mai, W. Sun, L. Xiong, Y. Liu, J. Ni, Chemosphere 73 (2008) 600.
[11] T. Karpova, S. Preis, J. Kallas, J. Hazard. Mater. 146 (2007) 465.
[12] Y. Zhang, J.L. Zhou, B. Ning, Water Res. 41 (2007) 19.
[13] H.M. Coleman, V. Vimonses, G. Leslie, R. Amal, Water Sci. Technol. 55 (2007) 301.
[14] E.J. Rosenfeldt, K.G. Linden, Environ. Sci. Technol. 38 (2004) 5476.
[15] H.M. Coleman, E.J. Routledge, J.P. Sumpter, B.R. Eggins, J.A. Byrne, Water Res. 38 (2004) 3233.
[16] B. Liu, X. Liu, Sci. Total Environ. 320 (2004) 269.
[17] X.L. Liu, F. Wu, N.S. Deng, Environ. Pollut. 126 (2003) 393.
[18] B. Liu, F. Wu, N.-S. Deng, J. Hazard. Mater. B98 (2003) 311.

[19] T. Nakashima, Y. Ohko, Y. Kubota, A. Fujishima, J. Photochem. Photobiol. A: Chem. 160 (2003) 115.
[20] T. Nakashima, Y. Ohko, D.A. Tryk, A. Fujishima, J. Photochem. Photobiol. A: Chem. 151 (2002) 207.
[21] Y. Ohko, K.-I. Iuchi, C. Niwa, T. Tatsuma, T. Nakashima, T. Iguchi, Y. Kubota, A. Fujishima, Environ. Sci. Technol. 36 (2002) 4175.
[22] H.M. Coleman, B.R. Eggins, J.A. Byrne, F.L. Palmer, E. King, Appl. Catal. B: Environ. 24 (2000) L1.
[23] A. Gora, B. Toepfer, V. Puddu, G. Li Puma, Appl. Catal. B: Environ. 65 (2006) 1.
[24] G. Li Puma, J.N. Khor, A. Brucato, Environ. Sci. Technol. 38 (2004) 3737.
[25] B. Toepfer, A. Gora, G. Li Puma, Appl. Catal. B: Environ. 69 (2007) 273.
[26] G. Li Puma, A. Brucato, Catal. Today 122 (2007) 78.
[27] R.J. Brandi, M.A. Citroni, O.M. Alfano, A.E. Cassano, Chem. Eng. Sci. 58 (2003) 979.
[28] A.E. Cassano, O.M. Alfano, Catal. Today 58 (2000) 167.
[29] A. Brucato, A.E. Cassano, F. Grisafi, G. Montante, L. Rizzuti, G. Vella, AIChE J. 52 (2006) 3882.
[30] J. Colina-Marquez, F. Machuca-Martinez, G. Li Puma, Environ. Sci. Technol. 43 (2009) 8953.
[31] G. Li Puma, B. Toepfer, A. Gora, Catal. Today 124 (2007) 124.
[32] R. Siegel, J.R. Howell, Thermal Radiation Heat Transfer, McGraw-Hill, London, 1972.
[33] M.L. Satuf, R.J. Brandi, A.E. Cassano, O.M. Alfano, Ind. Eng. Chem. Res. 44 (2005) 6643.
[34] S.M. Jacob, J.S. Dranoff, Chem. Eng. Prog. Symp. Ser. 62 (1966) 47.
[35] G. Li Puma, P.L. Yue, Chem. Eng. Sci. 58 (2003) 2269.
[36] P.M. Mazellier, L. Meite, J. De Laat, Chemosphere 73 (2008) 1216.